Transmission of Trans Effects in Dinuclear Complexes

Eduardo Sola, Francisco Torres, M. Victoria Jiménez, Jose A. López, Silvia E. Ruiz, Fernando J. Lahoz, Anabel Elduque, and Luis A. Oro*

Contribution form the Departamento de Quimica Inorgánica, Instituto de Ciencia de Materiales de Aragón, Universidad de Zaragoza-CSIC, 50009 Zaragoza, Spain

Received May 16, 2001

Abstract: The substitution of a terminal hydride ligand in the complexes $[Ir_2(\mu\text{-H})(\mu\text{-Pz})_2H_3(L)P^iPr_3)_2]$ (L = $NCCH_3$ (**1**) or pyrazole (**3**)) by chloride provokes a significant change in the lability of the L ligand, despite the fact that the substituted hydride and the L ligand lie in opposite extremes of the diiridium(III) complexes. Detailed structural studies of complex **3** and its chloro-trihydride analogue $[Ir_2(\mu\text{-H})(\mu\text{-Pz})_2H_2Cl(HPz)(P^iPr_3)_2]$ (**4**) have shown that this behavior is a consequence of the transmission of ligand trans effects from one extreme of the molecule to the other, with the participation of the bridging hydride. Extended Hückel calculations on model diiridium complexes have suggested that such trans effect transmissions are due to the formation of molecular orbitals of σ symmetry extended along the backbones of the complexes. This is also an expected feature for metal−metal bonded complexes. The feasibility of the transmission of ligand trans effects and trans influences through metal−metal bonds and its relevance to the understanding of both the reactivity and structures of metal−metal bonded dinuclear compounds have been substantiated through structural studies and selected reactions of the diiridium(II) complexes $[Ir_2(\mu\text{-1,8-}(NH)_2naphth)I(CH_3)(CO)_2(P^iPr_3)_2]$ (isomers **6** and **7**) and their cationic derivatives $[Ir_2(\mu\text{-1,8-}(NH)_2naphth)(CH_3)(CO)_2(P^iPr_3)_2](CF_3SO_3)$ (isomers **8** and **9**).

Introduction

The cooperative reactivity of the metal centers in dinuclear and polynuclear compounds can drive unique chemistry and catalysis.[1] This cooperation can arise from the proximity of the metal centers, which may favor the formation of metal−metal bonds or interactions and the existence of multimetallic coordination and reaction sites. Such features can bring advantageous mechanistic alternatives for substrate activation and subsequent reactions,[2] thus leading to unusual reactivities or enhanced catalytic activities. However, along with the species having close metal centers, other dinuclear species with related but distant metals can also exhibit cooperative reactivity.[3] It has been shown that distant metal centers can "talk to each other" via the bridging ligand system, through reorganizations in the ligands (mechanical coupling) or electronic influences (through-bond coupling).[4]

These latter cooperation pathways are different from those operating in compounds with close metal centers because they do not involve concerted actions of the various metal moieties on a substrate, but the transmission of information from one metal to another. The characterization of possible sources and mechanisms for such information transmission constitutes a challenge in the chemistry of polynuclear compounds, and may also enlighten the rational design of catalysts by exploiting cooperative reactivity.

Recently, we have reported on the reactivity of some diiridium(III) polyhydrides, which suggested that the trans effects of ligands could be transmitted from one metal center to another via hydride bridges.[5] Such transmission was inferred from the reactivity differences displayed by compounds **1** and **2** (Figure 1), since the substitution of the axial hydride of **1** by the less trans labilizing chloride ligand rendered the labile acetonitrile ligand at the other extreme of the molecule nonlabile. Further studies on the catalytic activity of complex **1** provided evidence for a dinuclear hydrogenation mechanism resulting from the facile migration of coordination vacancies along the dinuclear complex.[6] Such vacancy migrations could be understood as the result of ligand trans effects being transmitted from one side of the molecule to the other. These preliminary data, which have inspired the present study, strongly suggest the relevance of trans effect transmissions to cooperative reactivity and bimetallic catalysis. The selected examples of reactivity, structural data, and theoretical calculations on diiridium complexes discussed herein indicate that dinuclear trans effects and influences are not exclusive features of hydride-bridged complexes, and illustrate the potential importance of such concepts in the understanding of both the structure and reactivity of dinuclear compounds.

(1) (a) *Catalysis by Di- and Polynuclear Metal Cluster Complexes*; Adams, R. A., Cotton, F. A., Eds.; Wiley-VCH: New York, 1998. (b) Braunstein, P.; Rosé, J. In *Metal Clusters in Chemistry*; Braunstein, P., Oro, L. A., Raithby, P. R., Eds.; Wiley-VCH: Weinheim, Germany, 1999; p 616. (c) Van der Beuken, E. K.; Feringa, B. L. *Tetrahedron* **1998**, *54*, 12985.

(2) For some representative examples in dinuclear compounds, see: (a) Torkelson, J. R.; Antwi-Nsiah, F. H.; McDonald, R.; Cowie, M.; Pruis, J. G.; Jalkanen, K. J.; DeKock, R. L. *J. Am. Chem. Soc.* **1999**, *121*, 3666. (b) Torkelson, J. R.; McDonald, R.; Cowie, M. *J. Am. Chem. Soc.* **1998**, *120*, 4047. (c) Fryzuk, M. D.; Love, J. B.; Rettig, D. J.; Young, V. G. *Science* **1997**, *275*, 1445. (d) Tada, K.; Oishi, M.; Suzuki, H.; Tanaka, M. *Organometallics* **1996**, *15*, 2422. (e) Baranger, A. M.; Bergman, R. G. *J. Am. Chem. Soc.* **1994**, *116*, 3822. (f) Broussard, M. E.; Juma, B.; Train, S. G.; Peng, W. J.; Laneman, S. A.; Stanley, G. G. *Science* **1993**, *260*, 1784. (g) Fryzuk, M. D.; Piers, W. E. *Organometallics* **1990**, *9*, 986.

(3) (a) Zhang, X. X.; Wayland, B. *J. Am. Chem. Soc.* **1994**, *116*, 7897. (b) Esteruelas, M. A.; Garcia, M. P.; López, A. M.; Oro, L. A. *Organometallics* **1991**, *10*, 127.

(4) Bosnich, B. *Inorg. Chem.* **1999,** *38*, 2554.

(5) Sola, E.; Bakhmutov, V. I.; Torres, F.; Elduque, A.; López, J. A.; Lahoz, F. J.; Werner, H.; Oro, L. A. *Organometallics* **1998**, *17*, 683.

(6) Torres, F.; Sola, E.; Elduque, A.; Martinez, A. P.; Lahoz, F. J.; Oro, L. A. *Chem. Eur. J.* **2000**, *6*, 2120.

10.1021/ja016213l CCC: $20.00
Published on Web 11/02/2001

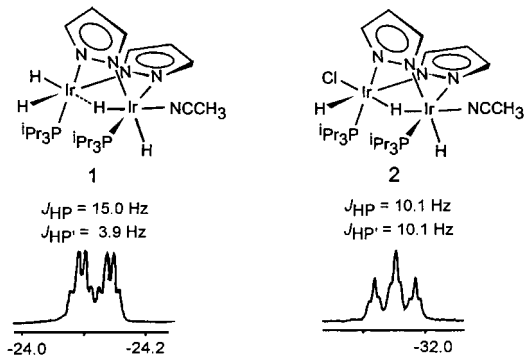

Figure 1. Proposed structures of the complexes $[Ir_2(\mu\text{-H})(\mu\text{-Pz})_2H_2X(NCCH_3)(P^iPr_3)_2]$ (X = H (**1**), Cl (**2**)) and their ^{1}H NMR signals corresponding to the bridging hydrides.

Scheme 1

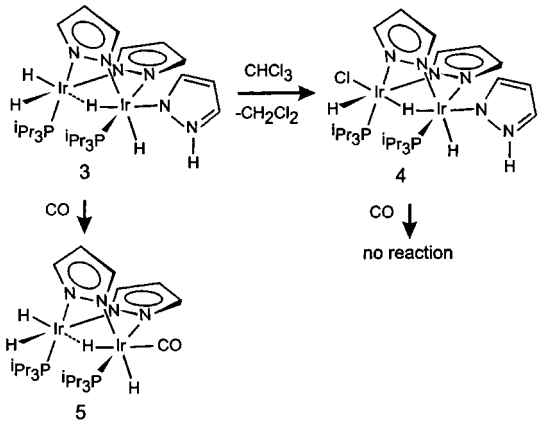

Results and Discussion

In our previous study of complexes **1** and **2**,[5] we proposed that the reactivity change induced by substitution of an axial hydride by chloride was accompanied by a subtle change in the position of the bridging hydride. Such a positional change, which suggested an active role of the bridge in the transmission of trans effects, was inferred from the ^{1}H NMR signals of the bridging hydrides shown in Figure 1. Thus, the signal for complex **2**, which shows two equal J_{HP} coupling constants, was consistent with a bridging hydride equidistant from both metal centers. In turn, the two different J_{HP} coupling constants observed in the corresponding signal of compound **1** suggested an asymmetric position for this hydride bridge. This proposal, attributing the different magnitude of the J_{HP} couplings to different H−Ir distances, could not be corroborated by the X-ray diffraction study of **1**, since the quality of its crystals was too low to allow the proper location and refinement of the hydrides.

Crystals of sufficient quality to accomplish such a study have been obtained for the related derivative $[Ir_2(\mu\text{-H})(\mu\text{-Pz})_2H_3(HPz)(P^iPr_3)_2]$ (**3**) (Scheme 1), the structure of which is shown in Figure 2. Even though hydride locations based on X-ray diffraction methods have to be considered with caution, the asymmetric position of the bridging hydride in this structural determination (Ir−H distances 1.61 and 2.00(7) Å) is consistent with the above-mentioned proposal since the NMR data of **3** are similar to those of **1**. A parallel structural study was attempted on the product resulting from the replacement of the axial hydride of **3** by chloride, the complex $[Ir_2(\mu\text{-H})(\mu\text{-Pz})_2H_2Cl(HPz)(P^iPr_3)_2]$ **(4)**, although in this case the low quality of the crystals and problems with disorder finally precluded the proper location of the hydrides. The structure of **4** depicted in Figure 2 shows the hydride ligands as positioned by the HYDEX program.[7] This structure was used as the starting point for a full-geometry optimization based on DFT calculations. For these calculations, the P^iPr_3 ligands were replaced by PH_3 groups with constrained rotation around the Ir−P axis. The distances of the complex backbone resulting from this optimization are shown below the X-ray structure of **4** in Figure 2, and are consistent with our proposal of a bridging hydride equidistant between the metals. A similar DFT optimization was carried out for the tetrahydride complex **3**, starting from a structure similar to that of **4** but replacing the chloride ligand by a hydride at a typical distance of 1.6 Å. These calculations converged to give the backbone distances depicted below the X-ray structure of **3** in Figure 2, which are consistent with those resulting from the X-ray structural determination (Table 1).

The structural results described above are also consistent with previous studies on other dinuclear compounds containing bridging hydrides. Similar nonsymmetric M(μ-H)M bridges have been found by X-ray diffraction in complexes such as $[Et_4N][Mo_2(\mu\text{-H})(CO)_9PPh_3]$[8] and $[Ru_2(\mu\text{-H})(\mu\text{-Pz})_2H(HPz)(cod)_2]$,[9] and by neutron diffraction analysis in the compound $[Pt_2(\mu\text{-H})H(dppe)_2]$.[10] In these examples, the bridging hydride coordinates trans to ligands having very different trans influences, hence accounting for the nonsymmetric position of the hydride. In agreement with this explanation, the neutron diffraction analysis of the complex $[Pt_2(\mu\text{-H})(Ph)_2(PMe_3)_4][BPh_4]$, in which the hydride coordinates trans to two phenyl ligands, revealed two equal Pt−H distances.[11] Furthermore, in the compound $[Pt_2(\mu\text{-H})(H)(Ph)_2(PMe_3)_2][BPh_4]$, with two good trans labilizing ligands (H and Ph) trans to the bridging hydride, two nearly equal Pt−H distances were observed by neutron diffraction.[12]

Compound **3** undergoes facile substitution of the pyrazole ligand by CO, to give the previously reported complex $[Ir_2(\mu\text{-H})(\mu\text{-Pz})_2H_3(CO)(P^iPr_3)_2]$ **(5)**.[5] The equivalent substitution in complex **4** is not observed even under harsh reaction conditions (Scheme 1). Given that such substitution reactions have been shown to follow dissociative mechanisms,[5] the reason for the different behavior of complexes **3** and **4** can be straightforwardly deduced from their X-ray structures, since the Ir−N(pyrazole) distance is considerably longer in complex **3** (Ir(1)−N(5) 2.142(4) Å) than in **4** (2.057(7) Å). The lengthening of the Ir−pyrazole bond in **3** (Figure 2) can be attributed to the sequential transmission of trans influence along the backbone of the complex. Thus, the larger trans influence of hydride compared to chloride pushes away the trans located bridging hydride, which consequently binds more strongly to the other iridium atom, and exerts a larger trans influence on the pyrazole ligand. From the kinetic point of view, this sequential transmission of trans influences results in the effective transmission of the hydride trans effect from one side of the molecule to the other.

This communication between metal centers can also be understood in terms of the molecular orbital schemes depicted in Figure 3. To offer the most simple and straightforward molecular orbital description of these compounds, calculations

(7) Orpen, A. G. *J. Chem. Soc., Dalton Trans.* **1980**, 2509.
(8) Darensbourg, M. Y.; Atwood, J. L.; Burch, R. R., Jr.; Hunter, W. E.; Walker, N. *J. Am. Chem. Soc.* **1979**, *101*, 2632.
(9) (a) Ashworth, T. V.; Liles, D. C.; Singleton, E. *J. Chem. Soc., Chem. Commun.* **1984**, 1317. (b) Albers, M. O.; Crosby, S. F. A.; Liles, D. C.; Robinson, D. J.; Shaver, A.; Singleton, E. *Organometallics* **1987**, *6*, 2014.
(10) Chiang, M. Y.; Bau, R.; Minghetti, G.; Bandini, A. L.; Banditelli, G.; Koetzle, T. F. *Inorg. Chem.* **1984**, *23*, 122.
(11) Albinati, A.; Chaloupka, S.; Eckert, J.; Venanzi, L. M.; Wolfer, M. K. *Inorg. Chim. Acta* **1997**, *259*, 305.
(12) Albinati, A.; Bracher, G.; Carmona, D.; Jans, J. H. P.; Klooster, W. T.; Koetzle, T. F.; Macchioni, A.; Ricci, J. S.; Thouvenot, R.; Venanzi, L. M. *Inorg. Chim. Acta* **1997**, *265*, 255.

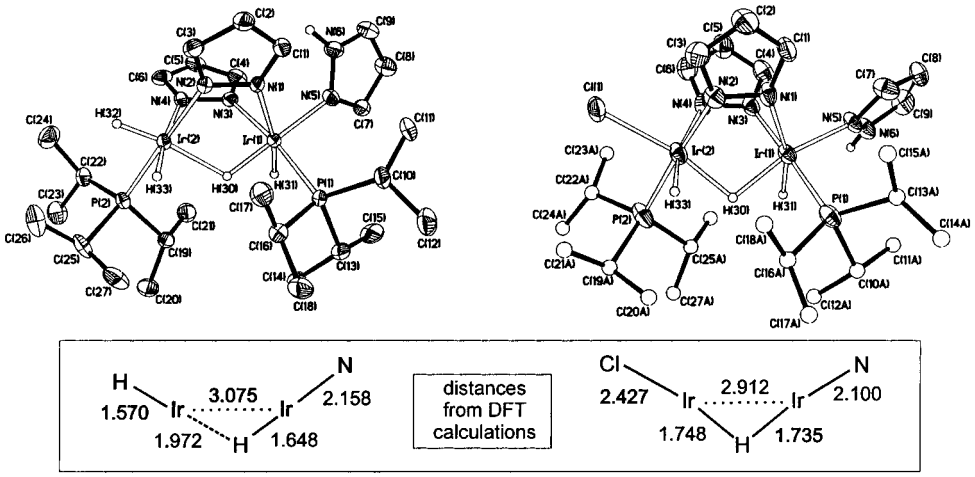

Figure 2. Molecular structures determined by X-ray diffraction of complexes **3** (left) and **4a** (right). Thermal ellipsoids are drawn at the 50% probability level. (Below) Bond distances (Å) involved in the backbones of the complexes obtained from DFT optimizations.

Table 1. Selected Crystallographic Bond Distances (Å) and Angles (deg) for Complexes **3** and **4a**[a]

	3	4a	4b
Ir(l)···Ir(2)	3.0413(7)	2.8784(8)	2.8793(8)
Ir(1)−P(1)	2.3090(16)	2.298(4)	2.288(4)
Ir(1)−N(1)	2.197(4)	2.164(9)	2.213(11)
Ir(1)−N(3)	2.123(4)	2.065(10)	2.081(10)
Ir(l)−N(5)	2.142(4)	2.060(9)	2.053(10)
Ir(1)−H(30)	1.61(7)		
Ir(l)−H(31)	1.53(7)		
Ir(2)−P(2)	2.2679(15)	2.284(4)	2.276(4)
Ir(2)−N(2)	2.127(5)	2.061(10)	2.088(10)
Ir(2)−N(4)	2.182(5)	2.143(10)	2.141(9)
Ir(2)−H(30)	2.00(7)		
Ir(2)−H(32)/C1	1.33(5)	2.390(3)	2.394(3)
lr(2)−H(33)	1.55(6)		
P(1)−Ir(1)−N(1)	98.11(13)	101.6(3)	102.0(3)
P(l)−Ir(l)−N(3)	172.22(13)	176.7(3)	175.7(3)
P(l)−Ir(l)−N(5)	101.20(14)	93.0(3)	93.2(3)
P(1)−Ir(1)−H(30)	85(2)		
P(1)−Ir(l)−H(3 1)	90(3)		
N(1)−Ir(1)−N(3)	86.55(18)	81.5(4)	81.0(4)
N(1)−Ir(1)−N(5)	92.56(17)	96.5(4)	97.5(4)
N(1)−Ir(1)−H(31)	168(3)		
N(3)−Ir(1)−N(5)	84.74(18)	87.8(4)	89.4(4)
N(5)−Ir(1)−H(30)	168(2)		
H(30)−Ir(1)−H(31)	75(3)		
P(2)−Ir(2)−N(2)	175.75(13)	174.9(3)	176.1(3)
P(2)−Ir(2)−N(4)	96.64(13)	102.3(3)	101.5(3)
P(2)−Ir(2)−H(30)	89(2)		
P(2)−Ir(2)−H(32)/Cl	83(2)	92.26(14)	91.85(13)
P(2)−Ir(2)−H(33)	85(2)		
N(2)−Ir(2)−N(4)	87.61(17)	82.2(4)	82.2(4)
N(2)−k(2)−H(32)/Cl	97(2)	89.8(3)	89.1(3)
N(4)−Ir(2)−H(32)/C1	98(2)	92.5(3)	93.0(3)
N(4)−Ir(2)−H(33)	173(2)		
H(30)−Ir(2)−H(32)	172(3)		
H(30)−Ir(2)−H(33)	90(3)		
H(32)−Ir(2)−H(33)	89(3)		
Ir(1)..Ir(2)−H(32)/Cl	159(2)	152.01(9)	152.80(9)
N(5)−Ir(1)..Ir(2)	145.18(13)	153.8(3)	155.9(3)

[a] **4a** and **4b** correspond to the two crystallographic independent molecules of **4.**

were carried out by extended Hückel methods[13] in linear model complexes containing only hydride and chloride ligands, since neither the bending of the molecule nor the charge of the compound influences the results of such calculations to a large extent. Figure 3 (left) represents the five σ molecular orbitals contributed by the ligands on the backbone of a symmetrical molecule with terminal chlorides and a bridging hydride. The three orbitals of lowest energy (1−3) are filled in the diiridium(III) complex. The replacement of one axial chloride by a hydride (Figure 3, center) substantially modifies the features of the filled orbitals 1 and 2, in a way that is consistent with our experimental observations. Thus, orbital 2, which does not involve the bridging hydride in the symmetric model, shows antibonding character at the position trans to the axial hydride in the asymmetric molecule. Consequently, a bonding contribution of similar magnitude appears at the other side of the bridging hydride. Also, the metal−axial ligand bonding contribution at the opposite extreme from the axial hydride disappears in orbital 1.

The above model calculations allow us to rationalize the experimentally observed transmission of trans effects as a consequence of the formation of σ molecular orbitals extended along the backbone of the dinuclear complex. However, these molecular orbitals are not an exclusive feature of complexes connected by bridging hydrides, being also present in more common types of compounds such as those containing metal−metal bonds. This observation is illustrated by the molecular orbital scheme depicted in Figure 3 (right), which has been calculated for a model metal−metal bonded diiridium(II) compound. The formal similarity between the molecular orbital descriptions of all those dinuclear species would suggest that the transmission of trans effects and influences could also affect the reactivity and structure of metal−metal bonded dinuclear complexes. Indeed, the transmission of trans influences through Au(II)−Au(II) bonds has been previously suggested to rationalize the structural features of bis(ylide) complexes containing L−Au−Au−L′ backbones, since the Au−L bond distances of these compounds seem to be controlled by the trans influence of L′.[14]

An experimental system capable of illustrating the transmission of trans effects and influences and their consequences in metal−metal bonded complexes was found in the diiridium compounds depicted in Scheme 2. The complex $[Ir_2(\mu\text{-}1,8\text{-}(NH)_2naphth)I(CH_3)(CO)_2(P^iPr_3)_2]$ **(6)** has been recently reported to be the kinetic product of methyl iodide oxidative addition to the diiridium(I) complex $[Ir_2(\mu\text{-}1,8\text{-}(NH)_2naphth)(CO)_2(P^i$-

(13) (a) Hoffmann, R. *J. Chem. Phys.* **1963**, *39*, 1397. (b) Hoffmann, R.; Lipscomb, W. N. *J. Chem. Phys.* **1962**, *36*, 2179. (c) Hoffmann, R.; Lipscomb, W. N. *J. Chem. Phys.* **1962**, *36*, 2872.

(14) (a) Murray, H. H.; Fackler, J. P., Jr.; Trzcinska-Bancroft, B. *Organometallics* **1985**, *4*, 1633. (b) Laguna, A.; Laguna, M.; Jiménez, J.; Lahoz, F. J.; Olmos, E. *J. Organomet. Chem.* **1992**, *435*, 235.

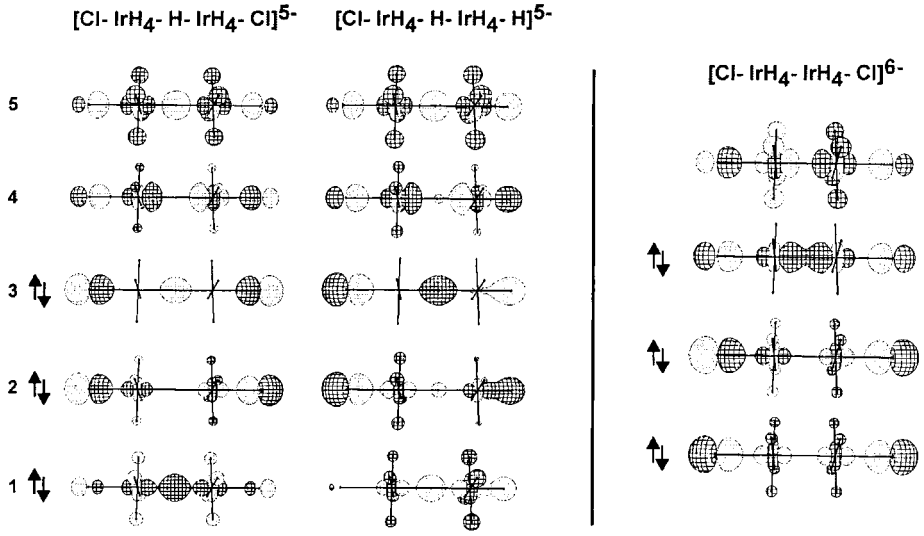

Figure 3. Molecular orbitals obtained by extended Hückel calculations on some model diiridium complexes: (left) symmetric and hydride bridged diiridium(III), (center) asymmetric with axial and bridging hydrides diiridium(III), (right) symmetric metal−metal bonded diiridium(II).

Scheme 2

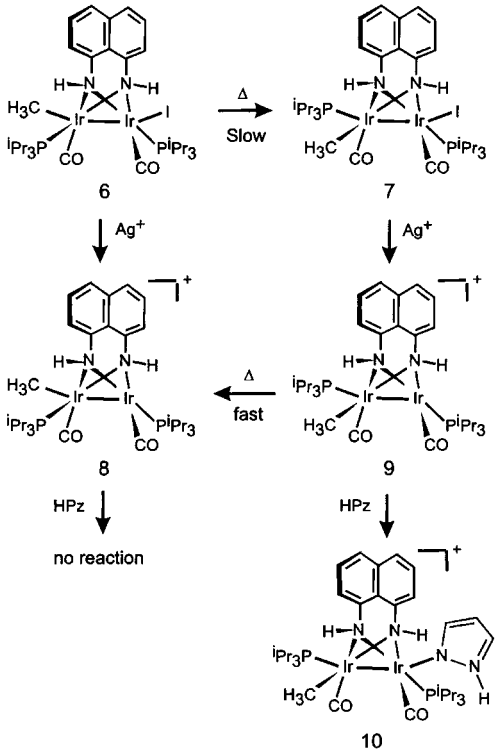

$Pr_3)_2$].[15] Compound **6** was found slowly to isomerize in solution to give the thermodynamic product of the reaction, the isomer **7**. Iodide abstraction with silver triflate from these two isomers has allowed the isolation of two isomeric cationic compounds of formula $[Ir_2(\mu\text{-}1,8\text{-}(NH)_2naphth)(CH_3)(CO)_2(P^iPr_3)_2](CF_3SO_3)$ (**8**, **9**), the structures of which are shown in Figure 4. Handling of isomer **9** in solution required low temperature, since its isomerization to **8** was found to be fast at room temperature.

On the basis of previous studies on unsaturated compounds related to **8** and **9**,[15,16] these isomers should be described as Ir(III)−Ir(I) mixed valence compounds, in which the metal atoms are connected by a weak Ir(I)−Ir(III) dative metal−metal bond. The relative strength of this dative Ir−Ir bond could be rather different in isomers **8** and **9**, given the different intermetallic distances observed for the compounds (Table 2). This could be primarily attributed to the different trans influences of CH_3 and P^iPr_3 ligands, since a sterically induced lengthening of the intermetallic distance in **8** is unlikely for a transoid arrangement of the phosphine ligands. Moreover, the existence of any destabilizing contribution of steric origin in the structure of **8** would not be consistent with the fact that **8** is the thermodynamically stable isomer.

Isomers **8** and **9** offer an excellent system to compare the behavior of coordination vacancies subjected to nearly equal steric constraints but different electronic environments as a result of the different spatial distribution of the ligands around the neighboring metal atom. Such electronic effects did not affect the reactivity of the isomeric compounds toward a strong nucleophile such as iodide, which in both cases reformed the neutral precursors **6** and **7**. The electronic effects were apparent upon reaction with a weaker nucleophile such as pyrazole. Thus, isomer **9** readily formed the isolable pyrazole compound $[Ir_2(\mu\text{-}1,8\text{-}(NH)_2naphth)(CH_3)(HPz)(CO)_2(P^iPr_3)_2](CF_3SO_3)$ (**10**) (Scheme 2), whereas no evidence for adduct formation was observed in the solutions containing **8** and pyrazole, even at low temperature. The structure of **10** determined by X-ray diffraction is shown in Figure 5; relevant bond distances and angles are listed in Table 2. As expected from the long Ir−N(pyrazole) distance observed in this structure, 2.233(6) Å, compound **10** was found to be very labile, since its solutions slowly produced the unsaturated complex **8** and free pyrazole when warmed to room temperature.

The reactivity differences displayed by complexes **8** and **9** toward pyrazole can be rationalized in terms of the transmission, through the metal−metal bond, of the trans labilizing properties of the phosphine and methyl ligand, since the instability of the pyrazole adduct of **8** can be readily attributed to the larger trans influence expected for a methyl ligand. By extrapolation of what is often observed in mononuclear unsaturated compounds, it could be expected that good trans labilizing ligands direct the coordination vacancy to the trans position in the ground state structure of an unsaturated dinuclear complex. In agreement with

(15) Jiménez, M. V.; Sola, E.; Egea, M. A.; Huet, A.; Francisco, A. C.; Lahoz, F. J.; Oro, L. A. *Inorg. Chem.* **2000**, *39*, 4868.

(16) (a) Oro, L. A.; Sola, E.; López, J. A.; Torres, F.; Elduque, A.; Lahoz, F. J. *Inorg. Chem. Commun.* **1998**, *1*, 64. (b) Jiménez, M. V.; Sola, E.; López, J. A.; Lahoz, L. A. *Chem. Eur. J.* **1998**, *4*, 1396. (c) Jimenez, M. V.; Sola, E.; Martinez, A. P.; Lahoz, F. J.; Oro, L. A. *Organometallics* **1999**, *18*, 1125.

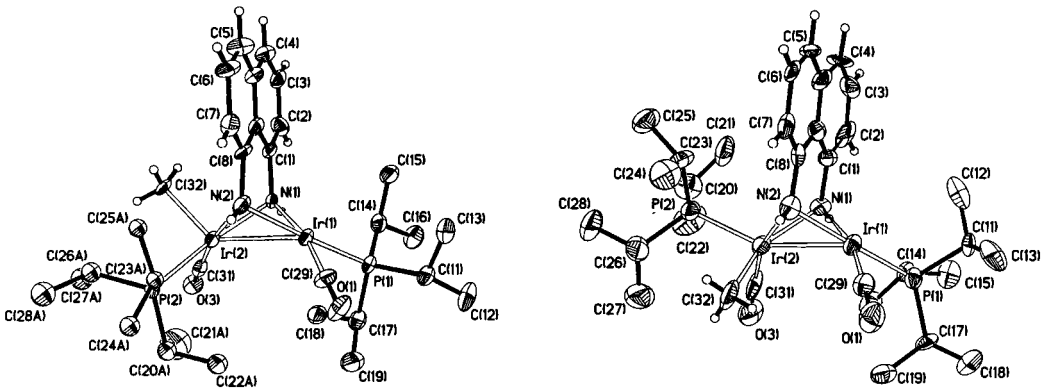

Figure 4. Molecular structures of the cations of complexes **8** (left) and **9a** (right). Thermal ellipsoids are drawn at the 50% probability level.

Table 2. Selected Crystallographic Bond Distances (Å) and Angles (deg) for Complexes **8**−**10**[a]

	8	9a	9b	10
Ir(l)−Ir(2)	2.7243(8)	2.6209(7)	2.6127(7)	2.5766(5)
Ir(l)−P(1)	2.300(2)	2.288(4)	2.283(3)	2.311(2)
Ir(l)−N(1)	2.105(8)	2.124(8)	2.077(8)	2.142(6)
Ir(l)−N(2)	2.114(8)	2.064(9)	2.130(9)	2.136(6)
Ir(l)−N(3)				2.233(6)
Ir(l)−C(29)	1.831(10)	1.777(13)	1.746(13)	1.805(9)
Ir(2)−P(2)	2.343(3)	2.282(3)	2.287(3)	2.336(2)
Ir(2)−N(l)	2.121(7)	2.062(8)	2.141(8)	2.194(6)
Ir(2)−N(2)	2.085(9)	2.140(9)	2.050(7)	2.035(8)
Ir(2)−C(31)	1.877(15)	1.779(13)	1.787(15)	1.786(11)
lr(2)−C(32)	2.088(9)	2.062(11)	2.088(13)	2.113(7)
P(l)−Ir(l)−Ir(2)	125.85(7)	120.14(8)	127.07(8)	116.05(6)
P(l)−Ir(l)−N(1)	97.5(2)	170.3(2)	100.1(3)	101.96(19)
P(l)−Ir(l)−N(2)	171.6(2)	102.4(3)	174.4(2)	166.2(2)
P(l)−Ir(l)−N(3)				98.17(19)
P(l)−Ir(l)−C(29)	89.9(3)	90.4(4)	91.0(4)	86.3(3)
N(l)−Ir(l)−N(2)	74.2(3)	72.0(3)	74.3(3)	71.1(3)
N(l)−Ir(l)−N(3)				94.4(2)
N(l)−Ir(l)−C(29)	167.8(4)	94.6(5)	163.9(5)	159.9(3)
N(2)−Ir(l)−N(3)				94.4(3)
N(2)−Ir(1)−C(29)	98.4(4)	166.2(5)	94.6(4)	96.7(3)
N(3)−Ir(l)−Ir(2)				136.54(17)
N(3)−Ir(l)−C(29)				102.6(3)
C(29)−Ir(l)−Ir(2)	117.7(3)	116.2(4)	111.1(4)	105.4(3)
P(2)−Ir(2)−Ir(l)	119.66(7)	154.66(9)	153.62(8)	153.32(7)
P(2)−Ir(2)−N(l)	169.2(2)	105.8(2)	114.4(2)	111.11(17)
P(2)−Ir(2)−N(2)	97.9(2)	115.6(3)	105.3(3)	103.5(2)
P(2)−Ir(2)−C(31)	90.2(3)	90.8(4)	92.4(4)	92.6(3)
P(2)−Ir(2)−C(32)	93.3(3)	92.4(4)	91.3(3)	92.3(2)
N(1)−Ir(2)−N(2)	74.4(3)	71.7(3)	74.6(3)	71.9(2)
N(l)−Ir(2)−C(31)	96.5(4)	163.3(4)	99.2(5)	102.6(3)
N(1)−Ir(2)−C(32)	95.1(3)	89.3(4)	151.4(4)	152.8(3)
N(2)−Ir(2)−C(31)	169.1(4)	99.4(4)	162.3(5)	163.9(3)
N(2)−Ir(2)−C(32)	97.1(4)	149.2(4)	87.2(4)	89.7(3)
C(31)−Ir(2)−Ir(l)	119.5(3)	111.0(4)	110.4(4)	110.8(3)
C(31)−Ir(2)−C(32)	89.7(4)	92.2(4)	91.5(6)	89.6(3)
C(32)−Ir(2)−Ir(l)	133.5(3)	99.1(3)	100.8(3)	100.4(2)

[a] **9a** and **9b** correspond to the two crystallographic independent molecules of **9**.

this, complex **8**, with a mutually trans disposition of the methyl ligand and the vacancy, is the thermodynamic isomer of the unsaturated cation $[Ir_2([\mu\text{-}1,8\text{-}(NH)_2naphth)(CH_3)(CO)_2(P^iPr_3)_2]^+$.

Arguments similar to those presented above may help to rationalize the structure of **7** (Scheme 2), the thermodynamically stable isomer of the neutral complex $[Ir_2(\mu\text{-}1,8\text{-}(NH)_2naphth)I(CH_3)(CO)_2(P^iPr_3)_2]$. When the thermally induced isomerization of complex **6** into **7** was carried out in $CDCl_3$ or acetone-d_6, in the presence of a 10-fold excess of $[NBu_4]Br$, the reaction product consisted of a 1:10 mixture of isomer **7** and its isostructural bromide complex $[Ir_2(\mu\text{-}1,8\text{-}(NH)_2naphth)Br(CH_3)(CO)_2(P^iPr_3)_2]$ (**11**) (Scheme 3). Substitution of iodide by

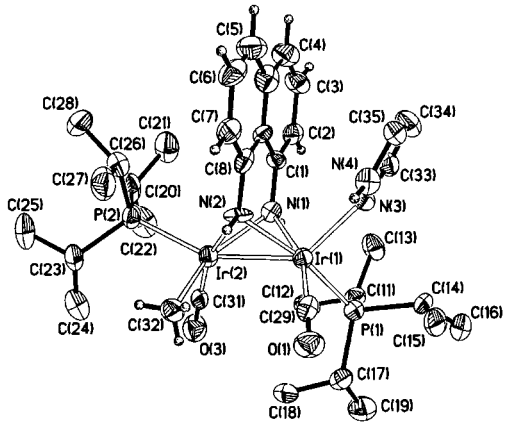

Figure 5. Molecular structure of the cation of complex **10**. Thermal ellipsoids are drawn at the 50% probability level.

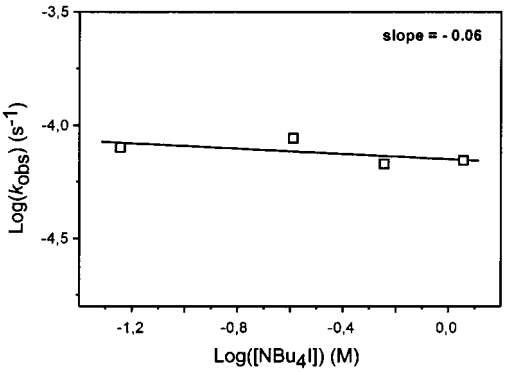

Figure 6. Dependence of the reaction rate upon iodide concentration for the isomerization of **6** into **7**.

Scheme 3

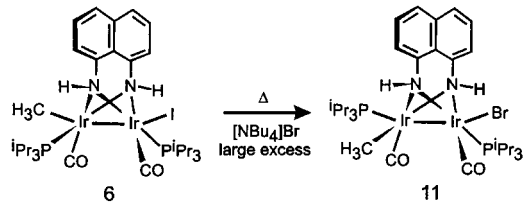

bromide in the precursor **6** was not observed during the reaction, suggesting that iodide dissociation is a necessary step within the isomerization mechanism. Pseudo-first-order rate constants for the isomerization of **6** into **7** (k_{obs}) were obtained by ^{31}P NMR spectroscopy at 328 K in the presence of different concentrations of $[NBu_4]I$, giving values around $7-8 \times 10^{-5}$ s^{-1}, irrespective of the complex/iodide ratio. This zero-order

Scheme 4

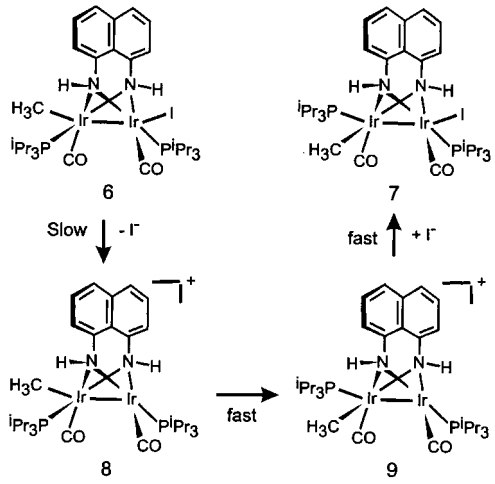

dependence upon iodide concentration (Figure 6) is consistent with the mechanism for isomerization of **6** to **7** depicted in Scheme 4. The intramolecular iodide dissociation from **6** is the initial and rate-determining step.

The mechanism shown in Scheme 4 together with the results discussed earlier, suggest that the transmission of trans effects and influences is the driving force for this isomerization reaction. Thus, isomerization would be favored by the lability of the iodide ligand of **6**, which is induced by the large trans effect of the methyl ligand. In turn, the smaller trans influence of the phosphine compared to that of methyl can account for the greater thermodynamic stability of isomer **7**.

Conclusion

The dinuclear compounds described in this paper together with their reactivity have revealed the feasibility of the transmission of ligand trans effects and influences along the backbone of dinuclear complexes. Such transmission probably occurs through molecular orbitals of σ symmetry extending along the dinuclear complexes, a situation that has been found to be favored by the presence of bridging hydrides or metal−metal bonds. This type of information transmission between metal centers allows the nature and spatial arrangement of the ligands coordinated to one metal to exert a profound influence upon the structure and reactivity of the neighboring metal containing fragment. In view of these results, we believe that these concepts of dinuclear trans effect and dinuclear trans influence may constitute useful tools for a better understanding of the chemistry of dinuclear compounds and, furthermore, to advance in the development of applications based on intermetallic cooperative reactivity.

Experimental Section

Physical Measurements. Infrared spectra were recorded as Nujol mulls on polyethylene sheets with use of a Nicolet 550 spectrometer. C, H, N, and S analyses were carried out in a Perkin-Elmer 2400 CHNS/O analyzer. NMR spectra were recorded on Varian UNITY, Varian Gemini 2000, or Bruker ARX, 300 MHz spectrometers. ^{1}H (300 MHz) and ^{13}C (75.19 MHz) NMR chemical shifts were measured relative to partially deuterated solvent peaks but are reported in ppm relative to tetramethylsilane. ^{31}P (121 MHz) NMR chemical shifts were measured relative to H_3PO_4 (85%). Coupling constants, *J*, are given in Hertz. Generally, spectral assignments were achieved by ^{1}H COSY, NOESY, and ^{13}C DEPT experiments. MS data were recorded on a VG Autospec double-focusing mass spectrometer operating in the positive mode; ions were produced with the Cs^+ gun at ca. 30 kV, and 3-nitrobenzyl alcohol (NBA) was used as the matrix. Conductivities were measured in ca. 3×10^{-4} M solutions with a Philips PW 9501/01 conductimeter.

Synthesis. All reactions were carried out with exclusion of air by using standard Schlenk techniques. Solvents were dried by known procedures and distilled under argon prior to use.[17] The complexes $[Ir_2(\mu\text{-H})(\mu\text{-Pz})_2H_3(HPz)(P^iPr_3)_2]$ (**3**)[5] and $[Ir_2(\mu\text{-1,8-(NH)}_2\text{naphth})I(CH_3)(CO)_2(P^iPr_3)_2]$ (isomers **6** and **7**)[15] were prepared by known procedures. All other reagents were obtained from commercial sources and were used as received. All the compounds whose preparations are described below are air sensitive in solution.

Preparation of $[Ir_2(\mu\text{-H})(\mu\text{-Pz})_2H_2Cl(HPz)(P^iPr_3)_2]$ (4). A solution of $[Ir_2(\mu\text{-H})(\mu\text{-Pz})_2H_3(HPz)(P^iPr_3)_2]$ (**3**) (100 mg, 0.11 mmol) in chloroform (2 mL) was heated for 30 min under reflux. The solvent was removed in vacuo, and the residue was treated with methanol to give a pale orange solid. The liquid phase was decanted, and the solid washed with methanol before drying in vacuo. Yield: 86 mg. Single crystals of **4** were grown from a concentrated chloroform solution, layered with hexane. Both the solid and the crystals gave microanalysis consistent with the presence of 1.5 molecules of $CHCl_3$ per molecule of **4**, just as found in the structural analysis by X-ray diffraction. Anal. Calcd for $C_{27}H_{55}ClIr_2N_6P_2\cdot1.5CHCl_3$: C, 30.44; H, 5.02; N, 7.47. Found: C, 30.04; H 5.31; N, 7.06. ^{1}H NMR (C_6D_6, 293 K) δ −32.98 (tt, $J_{HP} = J_{HP'} = 9.9$, $J_{HH} = J_{HH'} = 2.1$, 1H, Ir(μ−H)Ir), −21.86 (dd, $J_{HP} = 19.5$, $J_{HH} = 2.1$, 1H, IrH), −21.07 (dd, $J_{HP} = 18.5$, $J_{HH} = 2.1$, 1H, IrH), 0.85 (dd, $J_{HP} = 13.5$, $J_{HH} = 6.9$, 9H, PCHCH_3), 1.03 (dd, $J_{HP} = 12.9$, $J_{HH} = 7.2$, 9H, PCHCH_3), 1.06 (dd, $J_{HP} = 13.2$, $J_{HH} = 7.2$, 9H, PCHCH_3), 1.17 (dd, $J_{HP} = 12.9$, $J_{HH} = 7.2$, 9H, PCHCH_3), 2.23, 2.50 (both m, 3H, PCHCH_3), 5.83 (m, 2H, CH), 6.03 (dt, $J_{HP} = 1.8$, $J_{HH} = 1.5$, 1H, CH), 6.32 (dd, $J_{HH} = 2.7$, 2.1, 1H, CH), 7.45 (d, $J_{HH} = 2.7$, 1H, CH), 7.54 (m, 1H, CH), 7.76 (m, 1H, CH), 7.93 (d, $J_{HH} = 2.1$, 1H, CH), 8.06 (d, $J_{HH} = 1.8$, 1H, CH), 10.65 (br, 1H, NH). ^{31}P-{^{1}H} NMR (C_6D_6, 293 K) δ 4.28, 6.05 (both s).

Reactions of 3 and 4 with CO. Carbon monoxide was bubbled during ca. 2 min into solutions of the corresponding complex (ca. 20 mg) in $CDCl_3$ (0.5 mL), in an NMR tube, at room temperature. After this manipulation, the ^{1}H and ^{31}P {^{1}H} NMR of the samples were measured. The sample corresponding to the initial solution of complex **3** was completely transformed into a mixture of free pyrazole and a complex, which on the basis of its NMR features was identified as $[Ir_2(\mu\text{-H})(\mu\text{-Pz})_2H_3(CO)(P^iPr_3)_2]$ (**5**).[5] The sample corresponding to complex **4** only showed unreacted starting material. This sample was sealed under CO atmosphere and heated for 24 h at 333 K. After this period the only detectable complex in the solution was **4**.

Preparation of $[Ir_2(\mu\text{-1,8-(NH)}_2\text{naphth})(CH_3)(CO)_2(P^iPr_3)_2](CF_3SO_3)$ (8). The synthesis of this complex starting from the diiridium(I) compound $[Ir_2(\mu\text{-1,8-(NH)}_2\text{naphth})(CO)_2(PiPr_3)_2]$ has been previously described.[15] Alternatively, the complex can be obtained as follows: A Schlenk tube containing a solution of complex $[Ir_2(\mu\text{-1,8-(NH)}_2\text{naphth})I(CH_3)(CO)_2(P^iPr_3)_2]$ (isomer **6**) (200 mg, 0.19 mmol) in acetone (10 mL) was protected from the light and placed into a cooling bath at ca. 250 K. Silver triflate (49.5 mg, 0.19 mmol) was added to the solution, and the resulting suspension was stirred for 1 h. The suspension was filtered through Celite and the recovered solution was dried in vacuo to give a red oil. The oil was treated with diethyl ether to give a red solid, which was decanted, washed with ether and hexane, and dried in vacuo. Yield: 140 mg (75%). Single crystals of **8** were grown from acetone solutions, layered with diethyl ether. The microanalysis and NMR features of **8** in acetone-d_6 coincide with those already published.

Preparation of $[Ir_2(\mu\text{-1,8-(NH)}_2\text{naphth})(CH_3)(CO)_2(P^iPr_3)_2](CF_3SO_3)$ (9). The complex was prepared as a red solid (123 mg, 63% yield) following the procedure described for **8** but starting from complex **7**. Single crystals of **9** were grown from acetone solutions cooled at ca. 250 K, and layered with diethyl ether. Anal. Calcd for $C_{32}H_{53}F_3Ir_2O_5N_2P_2S$: C, 35.55; H, 4.94; N, 2.59. Found: C, 35.67; H, 5.03; N, 2.60. IR (cm^{-1}) 3310, 3281 ν(NH), 2010, 1983 ν(CO). MS (FAB+, *m*/*z* (%)) 932 (10) [M^+]. Λ_M (acetone) = 125 Ω^{-1} cm^2 mol^{-1} (1:1). ^{1}H

(17) (a) Shriver, D. F. *The Manipulation of Air-sensitive Compounds;* McGraw-Hill: New York, 1969. (b) Armarego, W. L. F.; Perrin, D. D. *Purification of Laboratory Chemicals*, 4th ed.; Butterworth-Heinmann; Oxford, 1996.

NMR (acetone-d_6, 293 K) δ 0.73 (dd, J_{HP} = 14.4, J_{HH} = 7.2, 9H, PCHCH_3), 1.13 (m, 3H, IrCH_3), 1.21 (dd, J_{HP} = 15.0, J_{HH} = 7.2, 9H, PCHCH_3), 1.30 (dd, J_{HP} = 14.0, J_{HH} = 6.9, 9H, PCHCH_3), 1.35 (dd, J_{HP} = 14.4, J_{HH} = 7.2, 9H, PCHCH_3), 2.77, 1.91 (both m, 3H, PCHCH_3), 6.84 (br, 1H, NH), 7.23 (t, J_{HH} = 7.9, 13 1H, CH), 7.29 (br, 1H, NH), 7.23 (t, J_{HH} = 7.9, 1H, CH), 7.47 (d, J_{HH} = 7.5, 1H, CH), 7.57 (d, J_{HH} = 8.1, 1H, CH), 7.71 (d, J_{HH} = 8.1, 1H, CH), 7.75 (d, J_{HH} = 7.5, I1H, CH). $^{31}P\{^1H\}$ NMR (acetone-d_6, 293 K) δ 42.82, 8.91 (both d, J_{PP} = 8.4). $^{13}C\{^1H\}$ NMR (acetone-d_6, 233 K) δ −19.70 (m, IrCH_3), 17.75 (d, J_{CP} = 3.8, PCHCH_3), 19.11, 19.69, 20.06 (all s, PCHCH_3), 24.18 (d, J_{CP} = 28.5, PCHCH_3), 25.46 (d, J_{CP} = 29.9, PCHCH_3), 112.21, 120.78 (both s, CH), 121.41 (s, C), 122.71, 127.78, 128.14 (all s, CH), 135.85 (s, C), 146.21 (d, J_{CP} = 2.4, C), 148.71 (m, C), 174.45 (d, J_{CP} = 7.9, CO), 177.24 (d, J_{CP} = 10.6, CO).

Preparation of [Ir$_2$(μ-1,8-(NH)$_2$naphth)(CH$_3$)(HPz)(CO)$_2$(P^{i}Pr$_3$)$_2$]-(CF$_3$SO$_3$) (10). A solution of **9** (100 mg, 0.09 mmol) in acetone (5 mL) was treated at ca. 250 K with pyrazole (6.47 mg, 0.09 mmol), and the mixture was stirred for 1 h. The resulting yellow solution was concentrated to ca. 0.5 mL and diethyl ether was added to produce a yellow precipitate. The solid was separated by decanting the solution, washed with diethyl ether, and dried in vacuo. Yield: 95 mg (72%). Single crystals of **10** were grown from acetone solutions cooled at ca. 250 K and layered with diethyl ether. Anal. Calcd for $C_{35}H_{57}F_3Ir_2N_4O_5P_2S$: C, 36.58; H, 5.00; N, 4.87; S, 2.79. Found: C, 36.98; H, 5.02; N, 5.10; S 2.69. IR (cm^{-1}) 3336, 3286, 3155 ν(NH), 1998, 1988 ν(CO). ^1H NMR (acetone-d_6, 293 K) δ 0.71 (dd, J_{HP} = 13.5, J_{HH} = 7.2, 9H, PCHCH_3), 1.14 (dd, J_{HP} = 13.2, J_{HH} = 6.9, 9H, PCHCH_3), 1.24 (d, J_{HP} = 2.4, 3H, IrCH_3), 1.35 (dd, J_{HP} = 14.7, J_{HH} = 7.5, 9H, PCHCH_3), 1.42 (dd, J_{HP} = 13.8, J_{HH} = 7.2, 9H, PCHCH_3), 1.84, 2.71 (both m, 3H, PCHCH_3), 5.83 (dd, J_{HH} = 2.4, 2.1, 1H, CH), 6.04, 6.48 (both br, 1H, NH), 7.05 (d, J_{HH} = 7.8, 1H, CH), 7.09 (d, J_{HH} = 7.2, 1H, CH), 7.15 (d, J_{HH} = 7.2, 1H, CH), 7.47 (m, 4H, CH), 7.67 (d, J_{HH} = 7.5, 1H, CH), 12.07 (m, 1H, NH). $^{31}P\{^1H\}$ NMR (acetone-d_6, 293 K) δ 26.23, −4.16 (both s). $^{13}C\{^1H\}$ NMR (acetone-d_6, 273 K) δ −24.76 (dd, J_{CP} = 8.7, 5.4, IrCH_3), 18.02 (d, J_{CP} = 3.7, PCHCH_3), 19.32 (d, J_{CP} = 2.3, PCHCH_3), 19.61, 20.13 (both s, PCHCH_3), 24.04 (d, J_{CP} = 24.9, PCHCH_3), 25.53 (d, J_{CP} = 29.0, PC*H*CH_3), 105.82, 111.65 (both s, CH), 113.02 (d, J_{CP} = 3.7, CH), 120.63 (s, CH), 121.42 (s, C), 121.57 (s, CH), 122.13 (q, J_{CF} = 320.4, CF_3SO_3), 127.64 (s, CH), 136.34 (s, C), 146.71 (d, J_{CP} = 2.7, C), 150.16 (d, J_{CP} = 2.3, C), 174.93 (dd, J_{CP} = 11.4, 1.9, CO), 177.70 (dd, J_{CP} = 8.2, 5.0, CO).

Isomerization of 6 into 7 in the Presence of [NBu$_4$]Br. An NMR tube containing a solution of complex **6** (20 mg, 0.019 mmol) and [NBu$_4$]Br (60.7 mg, 0.19 mmol) in acetone-d_6 (0.5 mL) was placed into an oil bath at 323 K. The course of the reaction was monitored by ^1H and $^{31}P\{^1H\}$ NMR over a period of 3 days. The starting complex **6** disappeared, giving rise to a mixture of **7** and a new complex **11** in a 1:10 molar ratio. No products other than **6**, **7**, and **11** were observed. Complex **11** was identified as the compound [Ir$_2$([μ-1,8-(NH)$_2$naphth)-Br(CH$_3$)(CO)$_2$(P^{i}Pr$_3$)$_2$], the bromide analogue of isomer **7**, on the basis of its NMR features and MS spectra. Data for **11**: MS (FAB+, *m*/*z* (%)) 1012 (10) [M$^+$]. ^1H NMR (acetone-d_6, 293 K) δ 0.28 (d, J_{HH} = 1.5, 3H, IrCH_3), 0.68 (dd, J_{HP} = 12.6, *JH* = 6.9, 9H, PCHCH_3), 1.09 (dd, J_{HP} = 14.4, J_{HH} = 6.9, 9H, PCHCH_3) [18H, PCHCH_3 and 3H, PCHCH_3 were hidden under the NBu$_4$ signals], 2.83 (m, 3H, PCHCH_3), 5.36, 5.76 (both br, 1H, NH), 6.98 (dd, J_{HH} = 8.1, 7.5, 1H, CH), 7.06 (dd, J_{HH} = 7.5, 6.9, 1H, CH), 7.18 (d, J_{HH} = 6.9, 1H, CH), 7.40 (d, J_{HH} = 8.1, 1H, CH), 7.48 (d, J_{HH} = 7.5, 1H, CH), 7.52 (d, J_{HH} = 7.5, 1H, CH). $^{31}P\{^1H\}$ NMR (acetone-d_6, 293 K) δ 23.36, −6.23 (both s).

Kinetics of Isomerization of 6 into 7. A solution of complex **6** in $CDCl_3$ (0.057 M) was prepared and stored at low temperature. Each sample was prepared by taking 0.5 mL of this solution into a NMR tube and dissolving the necessary amount of the soluble salt [NBu$_4$]I to obtain the desired iodide concentration. The decrease in the intensity of the $^{31}P\{^1H\}$ NMR signals of **6** was measured at intervals after the sample was stabilized at 328 K. The pseudo-first-order rate constants k_{obs} (s^{-1}) were obtained from the slopes of the plots of normalized signal integral vs time (s), under pseudo-first-order conditions (i.e. the first 10% of the reaction), using a least-squares approach. The values obtained were the following (k_{obs} (s^{-1})/[NBu$_4$]I concentration (M)): 7.97 E−5/0.052, 8.75 E−5/0.285, 6.75 E−5/0.57, 6.99 E−5/1.14. The experimental data used in these determinations are included in the Supporting Information.

Computational Experimental Details. The computational method used for geometry optimization of models of compounds **3** and **4** was density functional theory in its B3LYP formulation,[18] using the Gaussian98[19] series of programs. The basis sets used were the LanL2DZ effective core potential for iridium atoms: 6-31G** for chlorine, phosphorus and nitrogen atoms, and hydride ligands, and 6-31G for carbon and the rest of the hydrogen atoms. Calculations of the extended Hückel type[13] were carried out by using a modified version of the Wolfsberg−Helmholz formula.[20] The calculations and drawings were made with the program CACAO,[21] and the atomic parameters used are those implemented in this program.

Structural Analysis of Complexes 3, 4, 8, 9, and 10. X-ray data were collected for all complexes at low temperature (see crystal data below) on four-circle Siemens P4 (**3**) or Stoe-Siemens AED-2 diffractometers (**8**), or in a Bruker SMART APEX CCD diffractometer (**4**, **9**, and **10**) with graphite monochromated Mo Kα radiation (λ = 0.710 73 Å) using $\omega/2\theta$ (**3** and **8**) or ω scans (**4**, **9**, and **10**). Data were corrected for absorption by using a psi-scan method[22] (**3** and **8**) or a multiscan method applied with the SADABS program.[23]

The structures for all five compounds were solved by direct methods with SHELXS-86.[24] Refinement, by full-matrix least squares on F^2 with SHELXL97,[24] was similar for all complexes, including isotropic and subsequently anisotropic displacement parameters for all non-hydrogen nondisordered atoms. Particular details concerning the presence of solvent, static disorder, and hydrogen refinement are listed below. All the highest electronic residuals were observed in close proximity of the Ir centers and make no chemical sense.

Crystal data for 3: $C_{27}H_{56}Ir_2N_6P_2$, M = 911.12; colorless prismatic block, 0.38 × 0.26 × 0.20 mm^3; triclinic, $P\bar{1}$; a = 10.693(2) Å, b = 12.514(3) Å, c = 14.836(3) Å, α = 74.30(3)°, β = 75.73(3)°, γ = 69.95(3)°; Z = 2; V = 1769.2(6) Å^3; D_c = 1.710 g/cm^3; μ = 7.629 mm^{-1}, minimum and maximum transmission factors 0.1596 and 0.3107; $2\theta_{max}$ = 28.0°; temperature 123(1) K; 10325 reflections collected, 8398 unique [R(int) = 0.0452]; number of data/restrains/parameters 8398/0/457; final GoF 1.064, $R1$ = 0.0311 [6832 reflections, $I > 2\sigma(I)$], $wR2$ = 0.0714 for all data; largest difference peak 1.594 e·Å^{-3}; extinction coefficient 0.00069(8). Most of the hydrogen atoms were located in the difference maps; thus, pyrazole and pyrazolate hydrogens were refined as free isotropic atoms, while those of the phosphine ligands were refined by using a restricted riding mode. All the hydride ligands were located and refined in the last cycles of refinement as free isotropic atoms.

Crystal data for 4: $C_{27}H_{55}ClIr_2N_6P_2$·1.5$CHCl_3$, M= 1124.61; yellow irregular block, 0.35 × 0.31 × 0.25 mm^3; triclinic, $P\bar{1}$; a = 12.187(3) Å, b = 16.457(3) Å, c = 22.246(5) Å, α = 88.294(4)°, β = 83.524-(4)°, γ = 82.862(3)°; Z = 4; V= 4398.3(16) Å^3; D_c = 1.698 g/cm^3; μ = 6.478 mm^{-1}, minimum and maximum transmission factors

(18) (a) Becke, A. D. *J. Chem. Phys.* **1993**, *98*, 5648. (b) Lee, C.; Yang, W.; Parr, R. G. *Phys. Rev. B* **1998**, *37*, 785.

(19) Frisch, M. J.; Trucks, G. W.; Schlegel, H. B.; Scuseria, G. E.; Robb, M. A.; Cheeseman, J. R.; Zakrzewski, V. G.; Montgomery, J. A., Jr.; Stratmann, R. E.; Burant, J. C.; Dapprich, S.; Millam, J. M.; Daniels, A. D.; Kudin, K. N.; Strain, M. C.; Farkas, O.; Tomasi, J.; Barone, V.; Cossi, M.; Cammi, R.; Mennucci, B.; Pomelli, C.; Adamo, C.; Clifford, S.; Ochterski, J.; Petersson, G. A.; Ayala, P. Y.; Cui, Q.; Morokuma, K.; Malick, D. K.; Rabuck, A. D.; Raghavachari, K.; Foresman, J. B.; Cioslowski, J.; Ortiz, J. V.; Baboul, A. G.; Stefanov, B. B.; Liu, G.; Liashenko, A.; Piskorz, P.; Komaromi, I.; Gomperts, R.; Martin, R. L.; Fox, D. J.; Keith, T.; Al-Laham, M. A.; Peng, C. Y.; Nanayakkara, A.; Gonzalez, C.; Challacombe, M.; Gill, P. M. W.; Johnson, B.; Chen, W.; Wong, M. W.; Andres, J. L.; Head-Gordon, M.; Replogle, E. S.; Pople, J. A. *Gaussian 98*, Revision A.7; Gaussian, Inc.: Pittsburgh, PA, 1998.

(20) Ammeter, J. H.; Bdrgi, H. B.; Thibeault, J. C.; Hoffmann, R. *J. Am. Chem. Soc.* **1978**, *100*, 3686.

(21) Mealli, C.; Proserpio, D. M. *J. Chem. Edu.* **1990**, *67*, 399.

(22) North, C. T.; Phillips, D. C.; Mathews, F. S. *Acta Crystallogr.* **1986**, *A24*, 351.

(23) Blessing, R. H. *Acta Crystallogr.* **1995**, *A51*, 33−38. SADABS: Area-detector absorption correction, 1996, Bruker-AXS, Madison, WI.

(24) SHELXTL Package v. 6.10, 2000, Bruker-AXS, Madison, WI. Sheldrick, G. M. SHELXS-86 and SHELXL-97; University of Göttingen: Göttingen, Germany, 1997.

0.1867 and 0.3249; $2\theta_{max} = 27.0°$; temperature 173(2) K; 32072 reflections collected, 18706 unique [R(int) = 0.0531]; number of data/restrains/parameters 18706/172/768; final GoF 0.940, $R1 = 0.0628$ [10632 reflections, $I > 2\sigma(I)$], $wR2 = 0.1739$ for all data; largest difference peak 2.476 e·Å^{-3}. The crystal structure reveals the presence of three chloroform molecules of solvation together with the two independent dinuclear complexes; one chloroform molecule was observed disordered over two positions and was refined isotropically with complementary occupancies and geometric restrains. Additionally, three isopropyl groups of the phosphine ligands were also found to be disordered; they were refined with two isotropic models for each disordered moiety with fixed complementary occupancy. Hydrogens were only included for the pyrazole and pyrazolate ligands in calculated positions and were refined by using a riding model. The hydride ligands were included in the last cycles of refinement in the positions estimated from electrostatic potential calculations[7] and refined riding on Ir atoms.

Crystal data for 8: $C_{31}H_{53}ClIr_2N_2O_6P_2 \cdot C_3H_6O$, $M = 1089.62$; red prismatic block, 0.55 × 0.35 × 0.27 mm^3; monoclinic, $P2_1/c$; $a = 20.598(4)$ Å, $b = 12.756(3)$ Å, $c = 16.001(3)$ Å, $\beta = 110.03(2)°$; $Z = 4$; $V = 3949.9(14)$ Å^3; $D_c = 1.832$ g/cm^3; $\mu = 6.926$ mm^{-1}, minimum and maximum transmission factors 0.1148 and 0.2602; $2\theta_{max} = 25.1°$; temperature 100(1) K; 8693 reflections collected, 6931 unique [R(int) = 0.0541]; number of data/restrains/parameters 6931/1/459; final GoF 0.996, $R1 = 0.0459$ [5135 reflections, $I > 2\sigma(I)$], $wR2 = 0.1144$ for all data; largest difference peak 2.004 e·Å^{-3}; extinction coefficient 0.00013(5). The carbon atoms of one phosphine were found to be disordered and refined with isotropic displacement parameters; two models were included to take account of this disorder. All hydrogen atoms were included from calculated positions and refined riding on their corresponding C or N atoms. An acetone molecule of solvation was also found to be disordered in the asymmetric unit; two disordered models were included to complete one acetone molecule.

Crystal data for 9: $C_{32}H_{53}F_3Ir_2N_2O_5P_2S \cdot 0.5C_4H_{10}O$, $M = 1118.22$; red irregular block, 0.16 × 0.06 × 0.05 mm^3; triclinic, $P\bar{1}$; $a = 11.7846(11)$ Å, $b = 18.3407(18)$ Å, $c = 20.285(2)$ Å, $a = 100.799(2)°$, $\beta = 102.636(2)°$, $y = 102.471(2)°$; Z = 4; $V = 4048.5(7)$ Å^3; $D_c = 1.835$ g/cm^3; $\mu = 6.753$ mm^{-1}, minimum and maximum transmission factors 0.4113 and 0.7288; $2\theta_{max} = 28.8°$; temperature 173(2) K; 30883 reflections collected, 18373 unique [R(int) = 0.0891]; number of data/restrains/parameters 18373/21/949; final GoF 0.746, $R1 = 0.0568$ [7879 reflections, $I > 2\sigma(I)$], $wR2 = 0.0923$ for all data; largest difference peak 3.576 e·Å^{-3}. A diethyl ether molecule of solvation was detected and refined anisotropically. Hydrogen atoms were included from idealized positions and refined riding on their C or N atoms. No hydrogen was included for the solvent molecule.

Crystal data for 10: $C_{35}H_{57}F_3Ir_2N_4O_5P_2S \cdot 1.25\ C_4H_{10}O$, $M = 1241.90$; yellow irregular block, 0.22 × 0.18 × 0.17 mm^3; monoclinic, $P2_1/c$; $a = 11.8839(8)$ Å, $b = 19.9638(13)$ Å, $c = 20.7764(13)$ Å, $\beta = 91.4000(10)°$; $Z = 4$; $V = 4927.7(6)$ Å^3; $D_c = 1.674$ g/cm^3; $\mu = 5.560$ mm^{-1}, minimum and maximum transmission factors 0.3783 and 0.4463; $2\theta_{max} = 28.7°$; temperature 173(2) K; 32237 reflections collected, 11613 unique [R(int) = 0.0576]; number of data/restrains/parameters 11613/17/530; final GoF 0.992, $R1 = 0.0462$ [6955 reflections, $I > 2\sigma(I)$], $wR2 = 0.0926$ for all data; largest difference peak 3.205 e·Å^{-3}. Two molecules of diethyl ether were observed in the asymmetric unit. One of them was refined as a disordered molecule with two complementary moieties. For the second a partial occupation was assumed (0.25). Hydrogens in calculated positions were refined with a riding model.

Acknowledgment. We thank the Plan Nacional de Investigación, MCYT, for the support of this research (Project No. BQU2000-1170).

Supporting Information Available: Drawings and tables of atomic coordinates for the DFT-optimized structures of the PH_3 models for complexes **3** and **4**, and tables of $^{31}P\{^1H\}$ NMR signal integrals of **6** vs time and least-squares-fits used for the determination of complex **6** isomerization rates (PDF); an X-ray crystallographic file containing full details of the structural analysis of the five structures (CIF). This material is available free of charge via the Internet at http://pubs.acs.org.

JA016213L